

## SIMULATION OF INSTATIONARY, INCOMPRESSIBLE FLOWS

E. BÄNSCH

ABSTRACT. In this article a numerical method for the efficient simulation of instationary, viscous, incompressible flows in 2d and 3d is described. The time-discretization is based on the fractional step  $\theta$ -scheme in a variant as an operator splitting, which was introduced in [3].

### 1. INTRODUCTION

Consider the instationary Navier-Stokes equations in a bounded domain  $\Omega \subseteq \mathbb{R}^d$ ,  $d = 2$  or  $d = 3$ , with, say, Dirichlet boundary data  $u_D$  fulfilling  $\int_{\partial\Omega} u_D \cdot \nu = 0$ . That is we are looking for a pair  $(u, p)$  fulfilling

$$(1.1) \quad \begin{aligned} \partial_t u + u \cdot \nabla u - \frac{1}{Re} \Delta u + \nabla p &= f && \text{in } \mathbb{R}_+ \times \Omega, \\ \operatorname{div} u &= 0 && \text{in } \mathbb{R}_+ \times \Omega, \\ u &= u_D && \text{on } \mathbb{R}_+ \times \partial\Omega, \\ u(0, \cdot) &= u_0 && \text{in } \Omega. \end{aligned}$$

where

$$\begin{aligned} u: \mathbb{R}_+ \times \Omega &\longrightarrow \mathbb{R}^d && \text{is the (dimensionless) flow velocity,} \\ p: \mathbb{R}_+ \times \Omega &\longrightarrow \mathbb{R} && \text{is the (dimensionless) pressure,} \\ Re &= \frac{UL}{\nu} && \text{is the Reynolds number,} \end{aligned}$$

with  $L$  a length scale,  $U$  a typical velocity and the kinematic viscosity  $\nu$ .

For Reynolds numbers above a certain critical value (1.1) may be viewed as a complex dynamical system. A typical behavior of the solution to (1.1) with respect to the Reynolds number  $Re$  is the following, see for instance [10], [13]. Consider a situation which is stationary and virtually 2d with respect to the geometry and data, e.g. the situation depicted in Figure 1.

---

Received January 14, 1998.

1980 *Mathematics Subject Classification* (1991 *Revision*). Primary 35Q30, 65M60, 76D05.

*Key words and phrases*. Navier–Stokes equations, CFD, viscous incompressible flow, numerical solution, finite element method.

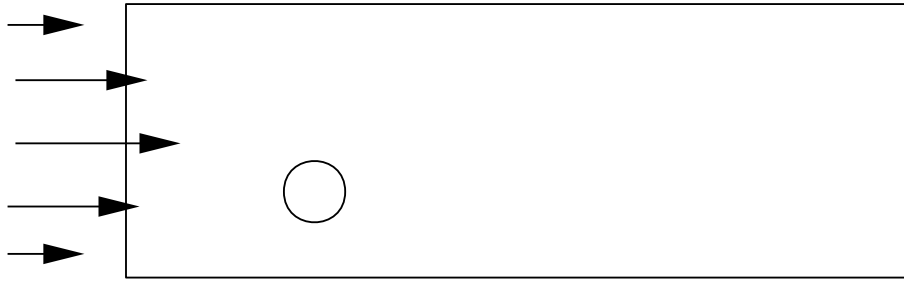


**Figure 1.** Model geometry, 2d clip into the 3d geometry.

Then usually for low Reynolds numbers, i.e. very viscous, laminar flows, one gets a 2d stationary solution. Increasing  $Re$  causes instability of the 2d solution and one gets a 3d solution. Further increase of  $Re$  results in a 3d time-dependent flow, the well known von-Karman vortex shedding, typically with a more complex temporal spectral distribution for higher  $Re$ . From a certain even higher value of  $Re$  one would expect turbulence, see Figure 2. This behavior is quite typical and may be expected in various other examples, see [7].

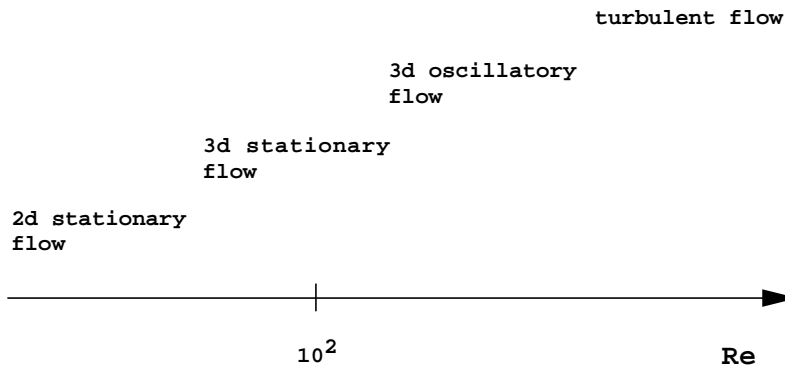


**Figure 2.** Behavior of the solution with respect to  $Re$ .

In many physical situations the transition from stationary to oscillatory and 2d to 3d is quite important. In particular the numerical determination of corresponding critical Reynolds numbers, where the transition takes place, as well as (temporal and spatial) frequencies and patterns of the solution are of great interest in applications. It turns out that commonly used simple time-discretization schemes like implicit Euler are often too dissipative to capture such features, see [10]. Thus the time discretization of (1.1) is quite crucial for an accurate Navier-Stokes solver.

Further major numerical problems arise due to:

- The incompressibility condition. Depending on the concrete situation this problem may be the most crucial and CPU-time consuming part of a Navier-Stokes solver.
- The strong nonlinearity. Most interesting phenomena in flow simulation result from strong nonlinear effects.
- The strong coupling of the unknowns in (1.1) by the solenoidal condition  $\operatorname{div} u = 0$  as well as by the nonlinear term  $u \cdot \nabla u$ .
- Stability versus accuracy. As already outlined we need a scheme, which is accurate to capture interesting phenomena (in time as well as in space), on the other hand the scheme has to have good stability properties.

Thus the requirements for a “good” Navier–Stokes solver are:

- stable, accurate, “efficient” time discretization,
- accurate spatial discretization,
- efficient solution of the fully discrete problems.

By “efficient” time discretization we mean that the resulting discretized systems should allow for an efficient solution technique.

We meet these requirements by using a solver which in an earlier version is described in [1] and has proved to be quite efficient in the range of moderate Reynolds numbers, see [13]. It is based on the techniques introduced in [3]. The time discretization is a variant of the so-called fractional step  $\theta$ -scheme and for the spatial discretization we use the **Taylor–Hood** element on unstructured simplicial grids in 2d and 3d, i.e. piecewise quadratics for the velocity and piecewise linears for the pressure.

The rest of this paper is organized as follows. In Section 2 we introduce an operator splitting by the fractional step  $\theta$ -scheme. This scheme reduces the Navier–Stokes system to two Stokes problems and a system of Burgers equations in each time step. In Sections 3 and 4 we propose methods how to solve these subproblems. Section 5 deals with the extension to convective energy transport. Some remarks on implementational aspects are given in Section 6. Finally we conclude the article by presenting some numerical examples in Section 7.

## 2. THE FRACTIONAL $\theta$ -SCHEME

As a model problem we consider formally the linear evolution equation

$$(2.2) \quad \begin{aligned} u_t + Au &= 0, \\ u(0) &= u_0 \end{aligned}$$

in a Banach space  $X$ . As pointed out above we are looking for a time discretization which is accurate, say of 2nd order, non-dissipative and  $A$ -stable. Commonly used simple schemes like implicit Euler or Crank–Nicolson method do not seem to be the method of choice. The implicit Euler method is strongly  $A$ -stable but first

order only and quite dissipative. The Crank–Nicolson scheme is of second order, non-dissipative but has only weak stability properties. Instead, we consider the so-called fractional step  $\theta$ -scheme, introduced for instance in [3].

For that let  $\theta = 1 - \frac{\sqrt{2}}{2} = 0.2928\dots$  and  $\alpha, \beta \in (0, 1)$ ,  $\alpha + \beta = 1$ ,  $\alpha > \frac{1}{2}$ . Split each time interval  $[t_n, t_{n+1}]$  into 3 subintervals  $[t_n, t_n + \theta\tau]$ ,  $[t_n + \theta\tau, t_n + (1 - \theta)\tau]$ , and  $[t_n + (1 - \theta)\tau, t_{n+1}]$  with  $\tau = t_{n+1} - t_n$ , see Figure 3.

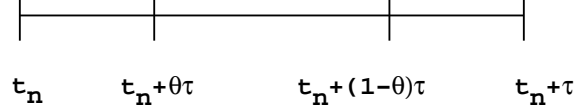


**Figure 3.** Split of  $[t_n, t_n + \tau]$  into 3 subintervals.

The fractional  $\theta$ -scheme is defined by: For  $n > 0$  find  $u^{n+\theta}, u^{n+1-\theta}, u^{n+1}$  such that  $u^0 = u_0$  and

$$(2.3) \quad \begin{aligned} \frac{u^{n+\theta} - u^n}{\theta\tau} + \alpha Au^{n+\theta} + \beta Au^n &= 0 \\ \frac{u^{n+1-\theta} - u^{n+\theta}}{(1-2\theta)\tau} + \beta Au^{n+1-\theta} + \alpha Au^{n+\theta} &= 0 \\ \frac{u^{n+1} - u^{n+1-\theta}}{\theta\tau} + \alpha Au^{n+1} + \beta Au^{n+1-\theta} &= 0 \end{aligned}$$

We define the corresponding damping factor  $\omega$  by

$$\omega(z) = \frac{(1 - \beta\theta z)^2(1 - \alpha(1 - 2\theta)z)}{(1 + \alpha\theta z)^2(1 + \beta(1 - 2\theta)z)}.$$

A spectral analysis shows that for  $A$  diagonalizable,  $\sigma(A) = \sigma_p(A) \subseteq \{z \in \mathbb{C} | \operatorname{Re} z \geq 0\}$  the scheme is unconditionally stable and of second order. The asymptotic damping factor fulfills  $\sup_{z \in \mathbb{R}_+} |\omega(z)| \leq 1$  and  $\lim_{z \rightarrow \infty} |\omega(z)| = \frac{\beta}{\alpha} < 1$  if  $\alpha > \frac{1}{2}$ . Furthermore we have  $|\omega(i\tau)| \approx 1$ , that means the scheme is nearly non-dissipative. Moreover if we choose  $\alpha = (1 - 2\theta)/(1 - \theta) = 0.5857\dots$  then all implicit operators in (2.3) are identical. See also [3], [9] for a more detailed discussion. In [9] one can also find a rigorous analysis of the fractional  $\theta$ -scheme for a class of nonlinear operators in a Hilbert space.

In [3] a variant of the fractional  $\theta$ -scheme is proposed as an operator splitting for the Navier–Stokes equations (1.1):

For  $n > 0$  find  $u^{n+\theta}, u^{n+1-\theta}, u^{n+1}$  and  $p^{n+\theta}, p^{n+1}$  such that

$$(2.4) \quad \left\{ \begin{aligned} \frac{u^{n+\theta} - u^n}{\theta\tau} - \frac{\alpha}{\operatorname{Re}} \Delta u^{n+\theta} + \nabla p^{n+\theta} &= f^{n+\theta} + \frac{\beta}{\operatorname{Re}} \Delta u^n \\ &\quad - (u^n \cdot \nabla) u^n \quad \text{in } \Omega, \\ \operatorname{div} u^{n+\theta} &= 0 \quad \text{in } \Omega, \\ u^{n+\theta} &= u_D^{n+\theta} \quad \text{on } \partial\Omega. \end{aligned} \right.$$

$$(2.5) \quad \begin{cases} \frac{u^{n+1-\theta} - u^{n+\theta}}{(1-2\theta)\tau} - \frac{\beta}{Re} \Delta u^{n+1-\theta} + (u^{n+1-\theta} \cdot \nabla) u^{n+1-\theta} \\ \quad \quad \quad = f^{n+1-\theta} + \frac{\alpha}{Re} \Delta u^{n+\theta} - \nabla p^{n+\theta} \quad \text{in } \Omega, \\ u^{n+1-\theta} = u_D^{n+1-\theta} \quad \text{on } \partial\Omega. \end{cases}$$

$$(2.6) \quad \begin{cases} \frac{u^{n+1} - u^{n+1-\theta}}{\theta\tau} - \frac{\alpha}{Re} \Delta u^{n+1} + \nabla p^{n+1} = f^{n+1} \\ \quad \quad \quad + \frac{\beta}{Re} \Delta u^{n+1-\theta} - (u^{n+1-\theta} \cdot \nabla) u^{n+1-\theta} \quad \text{in } \Omega, \\ \operatorname{div} u^{n+1} = 0 \quad \text{in } \Omega, \\ u^{n+1} = u_D^{n+1} \quad \text{on } \partial\Omega. \end{cases}$$

By (2.4)—(2.6) two major numerical difficulties of the Navier–Stokes equations, the treatment of the solenoidal condition and the nonlinearity, are decoupled. In (2.4) and (2.6) one has to solve a **linear, selfadjoint** Stokes system, the nonlinearity is treated explicitly. (2.5) is a Burgers like system of equations, the divergence free condition is dropped and the pressure gradient is taken from the previous time step. Thus by this operator splitting one reduces the Navier–Stokes equations to two considerably simpler subproblems. In [4], [6] conditionally stability and convergence for a fully discrete scheme is shown, in [9] the unconditionally stability and a (suboptimal) error estimate is stated for semi-discretization in time and the linear case. Our numerical experience is the following: Let  $Re \leq Re_*$  with  $Re_* \approx 10^3 - 10^4$  depending on the concrete problem. Then there exist  $h_*$  and  $\tau_*$  such that the scheme (2.4)—(2.6) is stable if  $h \leq h_*$  and  $\tau \leq \tau_*$ . Here  $h_* = h_*(x)$ ,  $h = h(x)$  denote functions describing the local mesh sizes for given triangulations.

### 3. SOLUTION OF THE STOKES PROBLEM

The Stokes subproblems (2.4), (2.6) may be written in the form (dropping subscripts for simplicity)

$$(3.7) \quad \begin{pmatrix} A(\gamma)B \\ B^T \quad 0 \end{pmatrix} \begin{pmatrix} u \\ p \end{pmatrix} = \begin{pmatrix} \tilde{f} \\ 0 \end{pmatrix},$$

where  $A(\gamma) := Id - \gamma\Delta$ ,  $\gamma := \frac{\theta\tau\alpha}{Re}$  and  $B := \nabla$ ,  $B^T = -\operatorname{div}$  and some right-hand side  $\tilde{f}$ . This system is equivalent to the **Schur complement** equation

$$(3.8) \quad T(\gamma)p := B^T A^{-1}(\gamma)Bp = B^T A^{-1}(\gamma)\tilde{f}$$

together with

$$A(\gamma)u = \tilde{f} - Bp.$$

Now for fixed  $\gamma > 0$  the Schur complement operator  $T(\gamma)$

$$T(\gamma): L^2(\Omega)_{/\mathbb{R}} \rightarrow L^2(\Omega)_{/\mathbb{R}}$$

is selfadjoint, positive definite and onto. Using a stable pair of finite element spaces  $V_h, W_h$  — for instance the Taylor–Hood element, see [5] — for the approximation of velocity and pressure respectively, i.e.  $V_h, W_h$  fulfill the Babuška-Brezzi condition uniformly in  $h$ , the above properties for  $T(\gamma)$  translate to  $T_h$ ,

$$T_h(\gamma): W_h \rightarrow W_h,$$

the discretized Schur complement operator, being symmetric, positive definite and having a bounded condition number independently of  $h$ . Thus a conjugate gradient method to solve (3.8) seems to be an optimal solver. However, for  $Re \rightarrow \infty$  or  $\tau \rightarrow 0$ , that is  $\gamma \rightarrow 0$ , the Schur complement degenerates and the condition number of  $T_h$  blows up. We expect a growth of

$$\text{cond}(T_h(\gamma)) = O\left(\frac{1}{h^2 + \gamma}\right)$$

in case of a quasi-uniform grid with mesh size  $h$ . Therefore we use a preconditioner  $S$  proposed in [3] given by

$$\begin{aligned} S: L^2(\Omega)_{/\mathbb{R}} &\rightarrow L^2(\Omega)_{/\mathbb{R}} \\ Sp &:= \gamma p + \varphi_p \end{aligned}$$

where  $\varphi_p$  is the unique solution of

$$\begin{aligned} -\Delta \varphi_p &= p && \text{in } \Omega, \\ \partial_\nu \varphi_p &= 0 && \text{on } \partial\Omega, \\ \int_\Omega \varphi_p &= 0. \end{aligned}$$

By Fourier analysis it is easy to see that  $S$  is the formal inverse of  $T$  in the case  $\Omega = \mathbb{R}^d$ .

Solving (3.8) by a CG with this preconditioner we get iteration numbers which are bounded independently of  $\gamma$  and  $h$  in practice. Note that the evaluation of  $S$  in the discrete case is inexpensive, since it involves only the inversion of a scalar Poisson problem. Furthermore the solution of this problem is sought in the pressure space  $W_h$  which is usually much smaller than the velocity space  $V_h$ .

## 4. SOLUTION OF THE NONLINEAR PROBLEM

To solve the nonlinear subproblem (2.5) we use a preconditioned GMRES method. Let us sketch the basic ideas of this method, see also for instance [8], [12].

For  $N \in \mathbb{N}$ ,  $M \in \mathbb{R}^{N \times N}$  regular,  $b \in \mathbb{R}^N$  consider the following linear problem in  $\mathbb{R}^N$ : Find  $x \in \mathbb{R}^N$  such that

$$Mx = b.$$

For a given  $k \in \mathbb{N}$  and an initial guess  $x_0 \in \mathbb{R}^N$  the GMRES algorithm determines an approximate solution  $\tilde{x} \in \mathbb{R}^N$  by

$$(4.9) \quad \tilde{x} = \arg \min_{z \in K} \|S(b - M(x_0 + z))\|_{\mathbb{R}^N}$$

with the Krylov space  $K := \text{span}\{Sr_0, SMr_0, \dots, SM^{k-1}r_0\}$ ,  $r_0 := S(b - Mx_0)$  the initial residual,  $\|\cdot\|_{\mathbb{R}^N}$  the Euclidean norm and  $S \in \mathbb{R}^{N \times N}$  a suitable preconditioner.

The minimization in (4.9) is based on finding an orthonormal basis of the space  $K$ . Usually the dimension  $k$  of the Krylov space  $K$  is chosen small and several restarts of GMRES are performed using the last iterate as initial value for the new start until the desired accuracy is achieved.

The nonlinear system of equations (2.5) may be written as

$$(4.10) \quad Au + N(u)u := \gamma_1 u - \gamma_2 \Delta u + u \cdot \nabla u = \tilde{f}$$

with  $N(v)w = v \cdot \nabla w$  and  $\gamma_1 := ((1 - 2\theta)\tau)^{-1}$ ,  $\gamma_2 := \frac{\beta}{Re}$  and  $\tilde{f}$  the right-hand side of (2.5). A variational formulation and discretization of (4.10) leads to a problem in  $\mathbb{R}^N$ ,  $N = \dim V_h$  the dimension of the discrete velocity space, of the form

$$(4.11) \quad A_h u_h + N_h(u_h)u_h = \tilde{f}_h,$$

where  $u_h \in \mathbb{R}^N$  is the vector of nodal values of the discrete solution in  $V_h$ . In order to apply the GMRES algorithm to (4.11) we freeze the nonlinearity  $N_h(\cdot)$  and update it at every restart. That is, in the  $p$ -th restart of GMRES we define

$$M := A_h + N_h(u_h^{p-1}),$$

where  $u_h^{p-1}$  is the  $(p-1)$ -th iterate and we set the initial guess  $u_{h,0}^p := u_h^{p-1}$ . It turns out that for transient flows a simple diagonal scaling as preconditioner  $S$  is sufficient. Moreover the dimension  $k$  of the Krylov space may be chosen quite small and the convergence of the method is rather fast, that means the number of restarts is small. Typical values for  $k$  are in the range of 10 – 25, the number of restarts usually lie between 4 – 10, even when the dimension  $N$  of the velocity space  $V_h$  is of the order  $10^5$ .

## 5. CONVECTIVE ENERGY TRANSPORT

In many applications heat transport by the flow field plays an important role. This transport is expressed by an advection-diffusion equation:

$$\partial_t \vartheta + u \cdot \nabla \vartheta - \frac{1}{RePr} \Delta \vartheta = 0 \quad \text{in } \Omega,$$

with  $\vartheta$  the dimensionless temperature and  $Pr$  the Prandtl number, which describes the relative influence of diffusive and convective transport. Of course, the above equation has to be closed by initial and boundary conditions, the latter ones for example of Dirichlet or Neumann type.

The influence of the temperature on the flow can often be modeled by the so called Boussinesq approximation. This model assumes the density to be constant except for the buoyancy terms. The momentum equation then reads:

$$\partial_t u + u \cdot \nabla u - \frac{1}{Re} \Delta u + \nabla p = - \frac{Gr}{Re^2} \vartheta \vec{g}$$

where  $\vec{g}$  denotes the direction of gravity and  $Gr$  the Grashof number, which describes the relative importance of the buoyancy forces with respect to the viscous forces.

In order to incorporate this model into the numerical scheme we propose a simple semi-implicit time-discretization: For  $n > 0$  find  $u^{n+\theta}, u^{n+1-\theta}, u^{n+1}$  and  $p^{n+\theta}, p^{n+1}$ , as well as  $\vartheta^{n+1}$  such that

$$\left\{ \begin{array}{l} \frac{u^{n+\theta} - u^n}{\theta\tau} - \frac{\alpha}{Re} \Delta u^{n+\theta} + \nabla p^{n+\theta} = \frac{\beta}{Re} \Delta u^n - (u^n \cdot \nabla) u^n \\ \quad - \frac{Gr}{Re^2} \vartheta^n \vec{g} \quad \text{in } \Omega, \\ \operatorname{div} u^{n+\theta} = 0 \quad \text{in } \Omega, \\ u^{n+\theta} = u_D^{n+\theta} \quad \text{on } \partial\Omega. \end{array} \right.$$

$$\left\{ \begin{array}{l} \frac{u^{n+1-\theta} - u^{n+\theta}}{(1-2\theta)\tau} - \frac{\beta}{Re} \Delta u^{n+1-\theta} + (u^{n+1-\theta} \cdot \nabla) u^{n+1-\theta} \\ \quad = \frac{\alpha}{Re} \Delta u^{n+\theta} - \nabla p^{n+\theta} - \frac{Gr}{Re^2} \vartheta^n \vec{g} \quad \text{in } \Omega, \\ u^{n+1-\theta} = u_D^{n+1-\theta} \quad \text{on } \partial\Omega. \end{array} \right.$$

$$\left\{ \begin{array}{l} \frac{u^{n+1} - u^{n+1-\theta}}{\theta\tau} - \frac{\alpha}{Re} \Delta u^{n+1} + \nabla p^{n+1} = \frac{\beta}{Re} \Delta u^{n+1-\theta} - (u^{n+1-\theta} \cdot \nabla) u^{n+1-\theta} \\ \quad - \frac{Gr}{Re^2} \vartheta^n \vec{g} \quad \text{in } \Omega, \\ \operatorname{div} u^{n+1} = 0 \quad \text{in } \Omega, \\ u^{n+1} = u_D^{n+1} \quad \text{on } \partial\Omega. \end{array} \right.$$

and

$$\frac{\vartheta^{n+1} - \vartheta^n}{\tau} + u^{n+1} \cdot \nabla \vartheta^{n+1} - \frac{1}{RePr} \Delta \vartheta^{n+1} = 0$$

+ boundary conditions.

This means we compute the new velocity and pressure with the buoyancy term given by the temperature from the previous time step and then determine the temperature on the new time step by using the new velocity. By this weak coupling the structure of the momentum equation is the same as for problem (1.1). Nevertheless, if one poses Dirichlet boundary condition for the velocity  $u$ , numerically this simple semi-implicit scheme is stable.

## 6. IMPLEMENTATIONAL ASPECTS

The method described in Sections 2–4 to solve problem (1.1) has been implemented in a FORTRAN code. The implementation has the following hierarchical structure, see Figure 4.

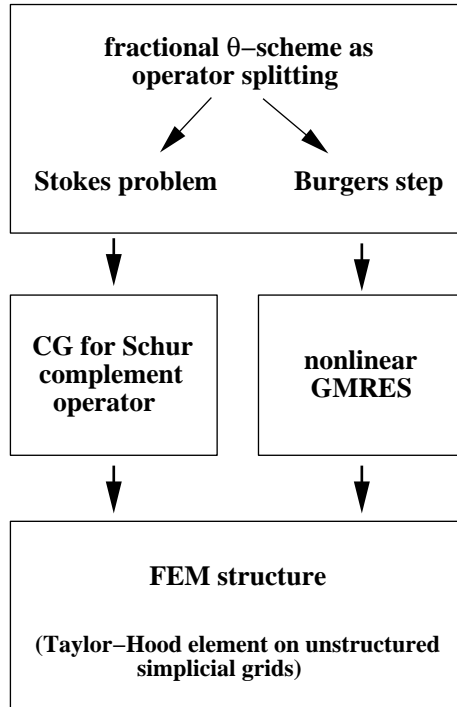


**Figure 4.** Structure of the Navier–Stokes solver.

The building blocks of the solver are virtually independent of each other. Thus an exchange of one or more modules is easy.

We summarize the main features of this code:

- 2d, 3d and 2.5d (i.e. rotationally symmetric data) solver for transient flow problems,
- time discretization by fractional step  $\theta$ -scheme as operator splitting,
- space discretization by Taylor–Hood element ( $\mathcal{P}_2 - \mathcal{P}_1$ ) on unstructured simplicial grids,
- incorporation of temperature equation in the Boussinesq approximation.

We also mention some functionality of the code which has not been addressed in this article:

- various boundary conditions (periodic, Neumann type, prescribed stresses),
- adaptivity in space (see [1]) and time possible,
- treatment of free capillary surfaces, see [2].

## 7. NUMERICAL RESULTS

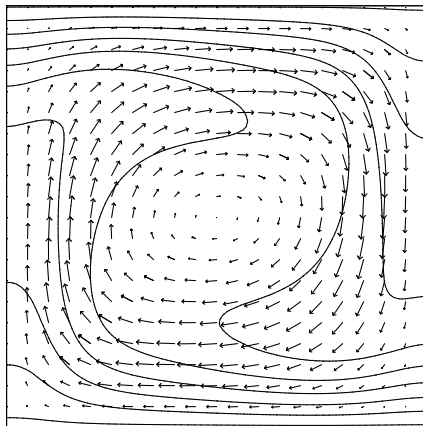


**Figure 5.** Stationary solution for  $Pr = 6.7$  and  $Ra = 5 \cdot 10^4$ ; velocity and isolines of the temperature.

As an example we consider a Bénard convection. We define  $\Omega = (0, 1) \times (0, 1)$ , impose homogeneous Dirichlet conditions for  $u$  on  $\partial\Omega$  and for the temperature  $\vartheta$  we set  $\vartheta = 1$  on the bottom,  $\vartheta = 0$  on the top and  $\partial_\nu \vartheta = 0$  on the side walls. Throughout the numerical experiments we set the Prandtl number to be that of water,  $Pr = 6.7$ .

Introducing the Rayleigh number  $Ra$  the Grashof number and the Reynolds number are given by

$$Gr = \frac{Ra}{Pr}, \quad Re = \sqrt{Gr}.$$

From a certain Rayleigh number  $Ra_1^* \approx 2.6 \cdot 10^3$  the static solution  $u \equiv 0$ ,  $\vartheta = 1 - x_2$  becomes unstable and one gets a stationary solution with one convection role, see Figure 5. At a second critical value  $Ra_2^* \approx 7.7 \cdot 10^4$  there is a transition to an oscillatory solution. In Figure 6 four time steps of the oscillatory solution are shown for  $Ra = 5 \cdot 10^5$ .

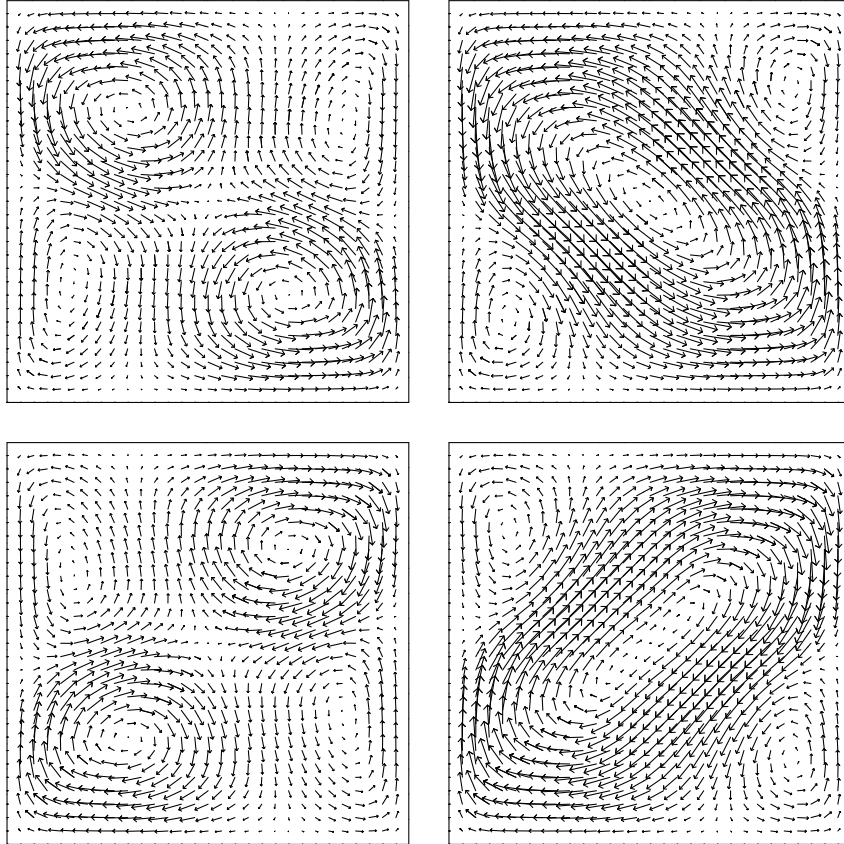


**Figure 6.** Velocity for  $t_1$ ,  $t_2 = t_1 + 3.6$ ,  $t_3 = t_1 + 16.0$  and  $t_4 = t_1 + 19.6$ ;  
 $Pr = 6.7$ ,  $Ra = 5 \cdot 10^5$ .

In order to study the time behavior of the system more quantitatively we fix a point  $x_0 \in \Omega$  and we look at the function  $t \mapsto Y(t, x_0)$ , where  $Y$  is some dependent variable. For  $x_0 = [0.25, 0.25]$  and  $Y = u_1$ ,  $u_1$  the first component of  $u$ , this function is plotted in Figure 7. The spectral power density function  $P$ , defined by

$$P(f) = |\mathcal{H}(f)|^2$$

with  $f$  the frequency and  $\mathcal{H}(f)$  the Fourier transform of  $Y$  given by

$$\mathcal{H}(f) = \int_{\mathbb{R}} Y(t, x_0) e^{2\pi i f t} dt,$$

clearly shows that in this example with  $Ra = 5 \cdot 10^5$  and  $Y = u_1$  there is one predominant frequency  $f = 0.035$ , see Figure 7 where  $P(f)/\max_f P(f)$  is plotted versus  $f$ . Figure 8 shows the result for  $Ra = 1.5 \cdot 10^6$ . In this case the solution is more involved and no longer periodical.

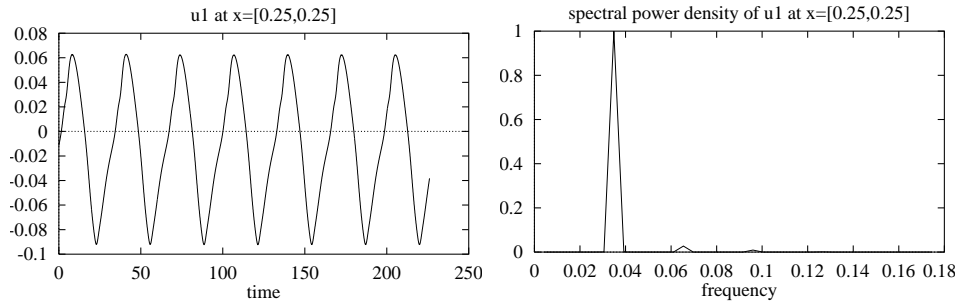


**Figure 7.**  $u_1$ -component of the velocity at  $x_0 = [0.25, 0.25]$  vs. time and spectral power density,  $Pr = 6.7$ ,  $Ra = 5 \cdot 10^5$ .

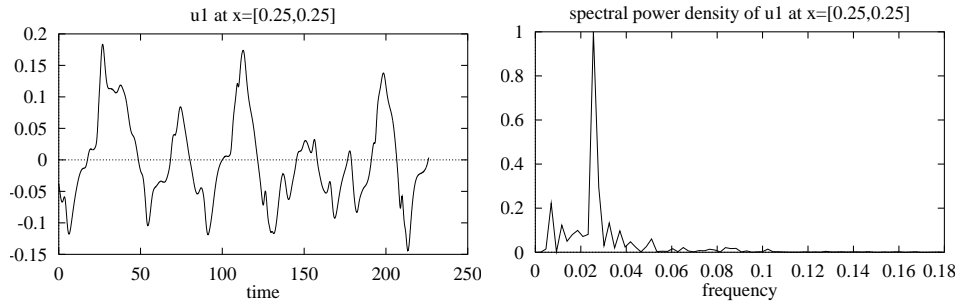


**Figure 8.**  $u_1$ -component of the velocity at  $x_0 = [0.25, 0.25]$  vs. time and spectral power density,  $Pr = 6.7$ ,  $Ra = 1.5 \cdot 10^6$ .

In 3D we consider an analogous example as in the 2D case.  $\Omega$  is now chosen to be a cylinder of height  $H = 1$  and radius  $R = 0.5$ . Again homogeneous Dirichlet conditions are imposed for  $u$  and the temperature fulfills  $\vartheta = 1$  on the bottom,  $\vartheta = 0$  on the top and  $\partial_\nu \vartheta = 0$  on the side walls.

Figures 9–11 show the complex behavior of the solution for  $Ra = 5 \cdot 10^5$ . In Figure 11  $Y$  is set  $Y = \vartheta$ .

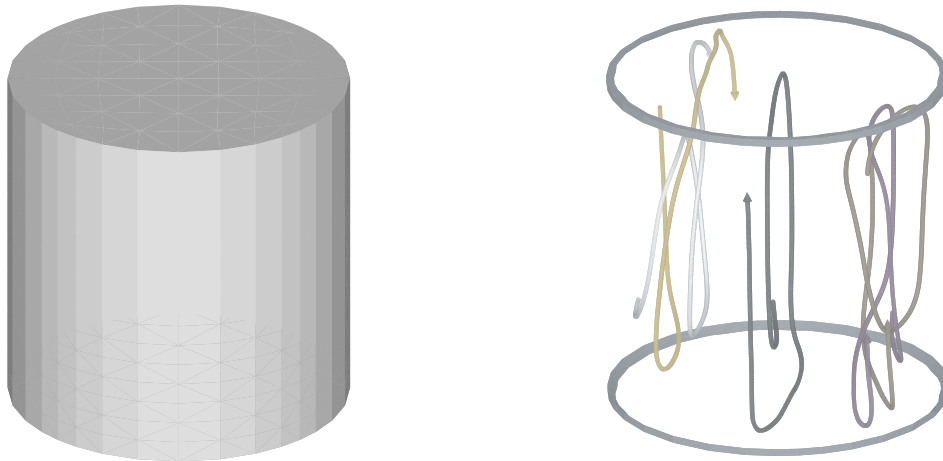


**Figure 9.** Geometry and flow visualization by particle tracing.

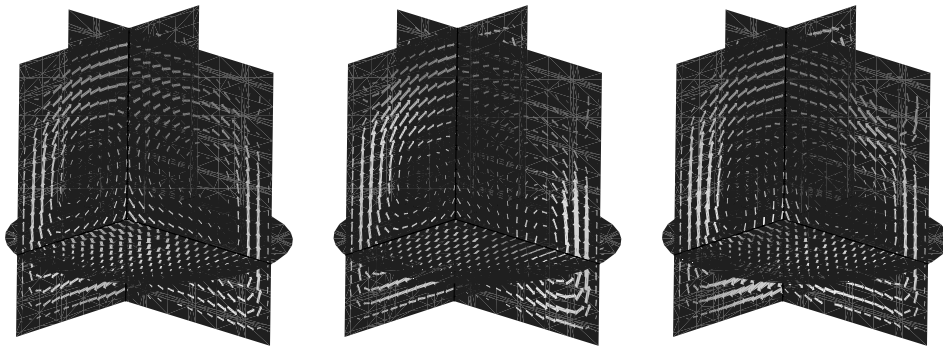


**Figure 10.** Velocity for  $t_1$ ,  $t_2 = t_1 + 26.0$  and  $t_3 = t_1 + 44.0$ .

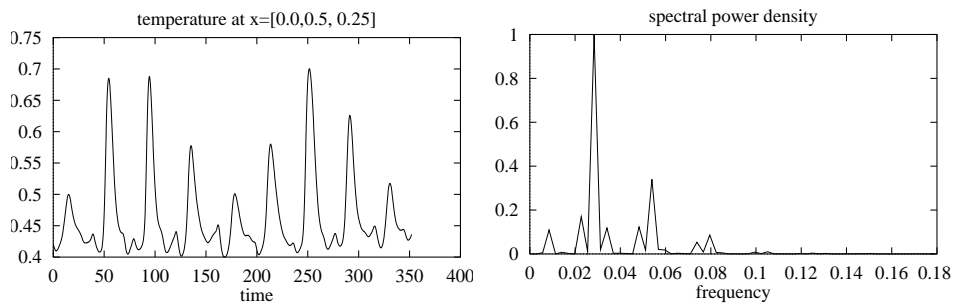


**Figure 11.** Temperature  $\vartheta$  at  $x_0 = [0.0, 0.5, 0.25]$  vs. time and spectral power density,  $Pr = 6.7$ ,  $Ra = 5 \cdot 10^5$ .

**Acknowledgment.** For the visualization of velocity and temperature fields the GRAPE visualization package was used, see [11].

### References

1. Bansch E., *An Adaptive Finite-Element-Strategy for the Three-Dimensional Time-Dependent Navier–Stokes Equations*, J. Comp. Appl. Math. **36** (1991), 3–28.
2. ———, *Numerical methods for the instationary Navier–Stokes equations with capillary free surface*, to appear.
3. Bristeau M. O., Glowinski R. and Periaux J., *Numerical methods for the Navier–Stokes equations. Application to the simulation of compressible and incompressible flows*, Computer Physics Report **6** (1987), 73–188.
4. Fernandez–Cara E. and Beltran M. M., *The Convergence of two Numerical Schemes for the Navier–Stokes Equations*, Numer. Math. **55** (1989), 33–60.
5. Girault V. and Raviart P. A., *Finite Element Methods for Navier–Stokes Equations, Theory and Algorithms*, Springer, Berlin – Heidelberg – New York – Tokyo, 1986.
6. Kloucek P. and Rys F., *Stability of the Fractional Step  $\theta$ -Scheme for the Nonstationary Navier–Stokes Equations*, SIAM J. Numer. Anal. **31**(5) (1994), 1312–1335.
7. Krishnamurti R., *Some further studies on the transition to turbulent convection*, J. Fluid Mech. **60** (1973), 285–303.
8. Mallet M., Periaux J. and Stoufflet B., *Convergence Acceleration of Finite Element Methods for the Solution of the Euler and Navier Stokes Equations of Compressible Flow*, Proceedings of the 7th GAMM-Conference on Numerical Methods in Fluid Mechanics Vieweg Notes on Numerical Fluid Mechanics (M. Deville, ed.), vol. 20, 1988.
9. Müller–Urbaniak S., *Eine Analyse des Zwischenschritt- $\theta$ -Verfahrens zur Lösung der instationären Navier–Stokes–Gleichungen*, Preprint 94-01 SFB 359, 1994.
10. Pironneau O., Rodi W., Ryhming I. L., Savill A. M. and Truong T. V. (eds.), *Numerical Simulation of Unsteady Flows and Transition to Turbulence*, Proceedings of the ERCOFTAC Workshop 1990,, Cambridge University Press, 1992.
11. Rumpf M. and Schmidt A. et al., *GRAPE, Graphics Programming Environment*, Report no. 8, SFB 256 Bonn, 1990.
12. Saad Y. and Schultz M. H., *GMRES: A Generalized Minimal Residual Algorithm for Solving Nonsymmetric Linear Systems*, SIAM J. Sci. Stat. Comput. **7**(3) (1986), 856–869.
13. Schäfer M. and Turek S., *Benchmark Computations of Laminar Flow Around a Cylinder, Flow Simulation with High–Performance Computers II*, Volume 52 of Notes on Numerical Fluid Mechanics, Vieweg (E. H. Hirschel, ed.), 1996, pp. 547–566.

E. Bansch, Inst. for Applied Mathematics, University of Freiburg, Germany